Frustration effects in antiferromagnetic face-centered cubic Heisenberg films

2007 J. Phys.: Condens. Matter 19 386202

(http://iopscience.iop.org/0953-8984/19/38/386202)

IOP PUBLISHING JOURNAL OF PHYSICS: CONDENSED MATTER

J. Phys.: Condens. Matter **19** (2007) 386202 (19pp) doi:10.1088/0953-8984/19/38/386202

Frustration effects in antiferromagnetic face-centered cubic Heisenberg films

V Thanh Ngo[2,3] **and H T Diep**[1,4]

[1] Laboratoire de Physique Théorique et Modélisation, CNRS-Université de Cergy-Pontoise, UMR 8089 2, Avenue Adolphe Chauvin, 95302 Cergy-Pontoise Cedex, France
[2] Institute of Physics, PO Box 429, Bo Ho, Hanoi 10000, Vietnam
[3] Asia Pacific Center for Theoretical Physics, Hogil Kim Memorial Building 5th floor, POSTECH, Hyoja-dong, Namgu, Pohang 790-784, Korea

E-mail: diep@u-cergy.fr

Received 9 May 2007, in final form 30 June 2007
Published 29 August 2007
Online at stacks.iop.org/JPhysCM/19/386202

Abstract

We study the effects of frustration in an antiferromagnetic film with a face-centered cubic (FCC) lattice structure with the Heisenberg spin model including an Ising-like anisotropy. Monte Carlo (MC) simulations have been used to study the thermodynamic properties of the film. We show that the presence of the surface reduces the ground state (GS) degeneracy found in the bulk. The GS is shown to depend on the surface in-plane interaction J_s with a critical value at which ordering of type I coexists with ordering of type II. Near this value a reentrant phase is found. Various physical quantities such as layer magnetizations and layer susceptibilities are shown and discussed. We study here how the physical properties vary as the surface bond strength changes at a fixed film thickness. The nature of the phase transition is also studied by a histogram technique. We have also used the Green's function (GF) method for the quantum counterpart model. The results at low temperature (T) show interesting effects of quantum fluctuations. Results obtained by the GF method at high T are compared to those of MC simulations. A good agreement is observed.

1. Introduction

Effects of the frustration in spin systems have been extensively investigated during the last 30 years. Frustrated spin systems are shown to have unusual properties such as large ground state (GS) degeneracy, additional GS symmetries, and successive phase transitions with complicated natures. Frustrated systems still challenge theoretical and experimental methods. For recent reviews, the reader is referred to [1].

[4] Author to whom any correspondence should be addressed.

On the other hand, during the same period the physics of surfaces and objects of nanometric size have also attracted an immense interest. This is due to important applications in industry [2–5]. In this field, results from laboratory research are often immediately used for industrial applications, without waiting for a full theoretical understanding. An example is the so-called giant magneto-resistance (GMR) used in data storage devices, magnetic sensors, etc [6–9]. In parallel to these experimental developments, much theoretical effort has also been devoted to the search of physical mechanisms lying behind new properties found in nanometric objects such as ultrathin films, ultrafine particles, quantum dots, spintronic devices, etc. This effort aimed not only at providing explanations for experimental observations but also at predicting new effects for future experiments [10, 11].

The aim of this paper is to investigate the effect of the presence of a film surface in a system which is known to be very frustrated, namely a face-centered cubic (FCC) antiferromagnet. The bulk properties of this material have been largely studied, as we will show below. In this paper, we would like to see in particular how the frustration effects on the nature of the phase transition in three dimensions are modified in thin films and how the surface conditions affect the magnetic phase diagram. We emphasize that we do not try to address how the physical properties vary as the film thickness changes. Rather we work with only one film thickness and address the question how a change in the surface bond strength changes the physical properties. We believe however that the effects obtained here remain generic when the film thickness varies. To carry out these purposes, we shall use Monte Carlo (MC) simulations and the Green's function (GF) method for qualitative comparison.

The paper is organized as follows. Section 2 is devoted to the description of the model. We recall there the properties of the three-dimensional (3D) counterpart model in order to better appreciate the properties of thin films obtained in this paper. A determination of its GS properties is also given. In section 3, we show our results obtained by MC simulations as functions of temperature T. The surface exchange interaction J_s is made to vary. A phase diagram in the space (T, J_s) is shown and discussed. In general, the surface transition is found to be distinct from the transition of interior layers. An interesting reentrant region is observed in the phase diagram. We also show in this section the results on the critical exponents obtained by the MC multihistogram technique. A detailed discussion on the nature of the phase transition is given. Section 4 is devoted to a study of the quantum version of the same model by the use of the GF method. We find interesting effects of quantum fluctuations at low T. The phase diagram (T, J_s) is established and compared to that obtained by MC simulations for the classical model. Concluding remarks are given in section 5.

2. Model and classical ground state analysis

It is known that the antiferromagnetic (AF) interaction between nearest-neighbor (NN) spins on the FCC lattice causes a very strong frustration. This is due to the fact that the FCC lattice is composed of corner-sharing tetrahedra, each of which has four equilateral triangles. It is well known [1] that it is impossible to fully satisfy simultaneously the three AF bond interactions on each triangle.

The analytical determination of the GS of systems of classical spins with competing interactions is a fascinating subject. For a recent review, the reader is referred to [12]. For a bulk FCC antiferromagnet, the Heisenberg spins on a tetrahedron form a configuration characterized by two arbitrary angles [13]. The ground state (GS) degeneracy is therefore infinite. This is also found in fully frustrated simple cubic lattice with classical Heisenberg spins [14]: the GS is also characterized by two random continuous parameters. To give an idea of the GS of a bulk FCC antiferromagnet [13], let us imagine two planes, xz and ψ, where ψ intersects with

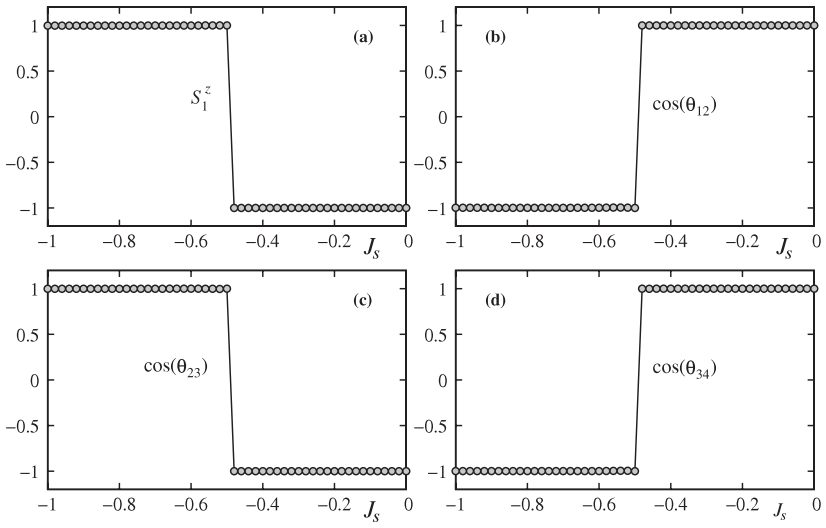

Figure 1. A ground state configuration of a single plaquette (a) S_1^z is S^z of sublattice 1, (b) $\cos\theta_{12}$, (c) $\cos\theta_{23}$, (d) $\cos\theta_{34}$. $\cos\theta_{ij}$ is the cosine of the angle between the two spins of sublattices i and j.

the xz plane along the z axis and makes an angle ϕ with the x axis. Two of the four spins make an angle θ in the xz plane symmetric with respect to the z axis. The other two spins make also the same angle, symmetric with respect to the z axis, but in the plane ψ. It has been shown [13] that the two angles θ and ϕ are arbitrary between 0 and π. Note that when $\theta = 0$ the spin configuration is collinear with two spins along the $+z$ axis and the other two along the $-z$ one. The phase transition of a bulk frustrated FCC Heisenberg antiferromagnet has been studied [15, 16]. In particular, the transition is found to be of the first order, as in the Ising case [17–19]. Other similar frustrated antiferromagnets such as the hexagon close-packed (HCP) antiferromagnet show the same behavior [20].

Let us consider a film of FCC lattice structure with [001] surfaces. To avoid the absence of long-range order of isotropic non Ising spin model at finite temperature (T) when the film thickness is very small, i.e. a quasi-two-dimensional system [21], we add in the Hamiltonian an Ising-like uniaxial anisotropy term. The Hamiltonian is given by

$$\mathcal{H} = -\sum_{\langle i,j\rangle} J_{i,j}\mathbf{S}_i \cdot \mathbf{S}_j - \sum_i D_i (S_i^z)^2, \tag{1}$$

where $\mathbf{S}_i$ is the Heisenberg spin at the lattice site i, and $\sum_{\langle i,j\rangle}$ indicates the sum over the NN spin pairs $\mathbf{S}_i$ and $\mathbf{S}_j$.

In the following, the interaction between two NN surface spins is denoted by J_s, while all other interactions are supposed to be antiferromagnetic and all equal to $J = -1$ for simplicity. Note that the case of pure Ising model on the simple cubic lattice has been studied by MC simulation with various surface conditions [22, 23].

We first determine the GS configuration by using the steepest descent method: starting from a random spin configuration, we calculate the magnetic local field at each site and align the spin of the site in its local field. In doing so for all spins and repeating until the convergence is reached, we easily obtain the GS configuration without metastable states. The result is shown in figure 1

We observe that there is a critical value $J_s^c = -0.5$. For $J_s < J_s^c$, the spins in each yz plane are parallel, while the spins in adjacent yz planes are antiparallel (figure 2(a)). This

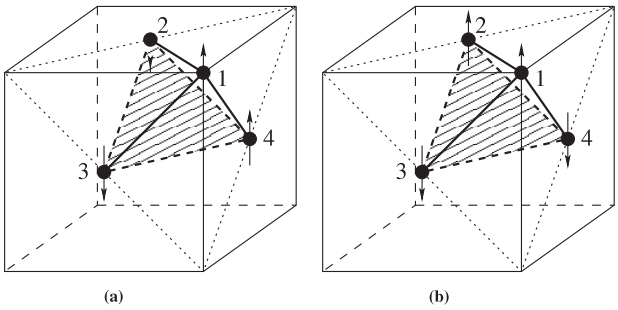

Figure 2. The ground state spin configuration of the FCC cell at the film surface: (a) ordering of type I for $J_s < -0.5$; (b) ordering of type II for $J_s > -0.5$.

ordering will be called hereafter 'ordering of type I': in the x direction the ferromagnetic planes are antiferromagnetically coupled, as shown in this figure. Of course, there is a degenerate configuration where the ferromagnetic planes are antiferromagnetically ordered in the y direction. Note that the surface layer has an AF ordering for both configurations. The degeneracy of type I is therefore 4, including the reversal of all spins.

For $J_s > J_s^c$, the spins in each xy plane are ferromagnetic. The adjacent xy planes have an AF ordering in the z direction perpendicular to the film surface. This will be called hereafter 'ordering of type II'. Note that the surface layer is then ferromagnetic (figure 2(b)). The degeneracy of type II is 2, due to the reversal of all spins.

Without using a general method [12, 13], let us calculate analytically the GS configuration in a simple manner for the present model.

Consider a tetrahedron with the spins numbered as in figure 2: S_1, S_2, S_3 and S_4 are the spins in the surface FCC cell (first cell). The interaction between S_1 and S_2 is set to be equal to J_s ($-1 \leqslant J_s \leqslant 0$) and all others are taken to be equal to J (< 0), and all $D_i = D$ for simplicity. The Hamiltonian for the cell is written as

$$H_p = -\tfrac{1}{2}\{8J_s(\mathbf{S}_1 \cdot \mathbf{S}_2) + 8J(\mathbf{S}_3 \cdot \mathbf{S}_4) + 6J\,[\mathbf{S}_1 \cdot \mathbf{S}_3 + \mathbf{S}_1 \cdot \mathbf{S}_4 + \mathbf{S}_2 \cdot \mathbf{S}_3 + \mathbf{S}_2 \cdot \mathbf{S}_4] + 2D[(S_1^z)^2 + (S_2^z)^2 + (S_3^z)^2 + (S_4^z)^2]\}. \tag{2}$$

Let us decompose each spin into two components: an xy component, which is a vector, and a z component $\mathbf{S}_i = (\mathbf{S}_i^{\parallel}, S_i^z)$. The numerical results shown above indicate that the spins have only a z component. Taking advantage of this, we suppose that the xy vector components of the spins are all equal to zero. The angles θ_i of $\mathbf{S}_i$ with the z axis are then

$$\theta_1 = 0, \qquad \theta_3 = \pi$$
$$\theta_2 = \beta_1, \qquad \theta_4 = \beta_2.$$

The total energy of the cell (2), with $S_i = \frac{1}{2}$, can be rewritten as

$$H_p = -\frac{D}{2} + \frac{3J}{4} + \left(\frac{3J}{4} - J_s - \frac{D}{4}\cos\beta_1\right)\cos\beta_1 + \frac{1}{4}(J - D\cos\beta_2)\cos\beta_2 - \frac{3J}{4}\cos\beta_1\cos\beta_2. \tag{3}$$

By a variational method, the minimum of the cell energy corresponds to

$$\frac{\partial H_p}{\partial \beta_1} = J_s \sin\beta_1 + \frac{D}{2}\cos\beta_1 \sin\beta_1 - \frac{3J}{4}\sin\beta_1 + \frac{3J}{4}\cos\beta_2 \sin\beta_1 = 0, \tag{4}$$

$$\frac{\partial H_p}{\partial \beta_2} = \left[\frac{3J}{4}\cos\beta_1 - \frac{J}{4} + \frac{D}{2}\cos\beta_2\right]\sin\beta_2 = 0. \tag{5}$$

The solutions of equations (4) and (5) corresponding to the minimal energy are

$$\begin{aligned} &\cos\beta_1 = -\cos\beta_2 = -1 \qquad \text{for } |J_s| > 0.5, \\ &\cos\beta_1 = -\cos\beta_2 = 1 \qquad \text{for } |J_s| < 0.5. \end{aligned} \tag{6}$$

Note that these solutions do not depend on D. The GS energy per spin is

$$\begin{aligned} &H_p = -D + J + J_s \qquad \text{for } |J_s| > 0.5, \\ &H_p = -D + 2J - J_s \qquad \text{for } |J_s| < 0.5. \end{aligned} \tag{7}$$

We see that the solution (6) agrees with the numerical result.

3. Monte Carlo results

In this section, we show the results obtained by MC simulations with the Hamiltonian (1). The spin model is the classical Heisenberg model of magnitude $S = 1$.

The film size is $L \times L \times N_z$, where N_z is the number of FCC cells along the z direction (film thickness). Note that each cell has two atomic planes. We use here $L = 12, 18, 24, 30, 36$ and $N_z = 4$. Periodic boundary conditions are used in the xy planes. The equilibrating time is about 10^6 MC steps per spin and the averaging time is 2×10^6 MC steps per spin. $|J| = 1$ is taken as unit of energy in the following.

Before showing the results let us adopt the following notation. The sublattice 1 of the first cell belongs to the surface layer, while the sublattice 3 of the first cell belongs to the second layer. The sublattices 1 and 3 of the second cell belong, respectively, to the third and fourth layers. In our simulations, we used four cells, $N_z = 4$, i.e. eight atomic layers. The symmetry of the two film surfaces imposes the equivalence of the first and fourth cells and that of the second and third cells. It suffices then to show results of the first two cells, i.e. the first four layers. In addition, in each atomic layer the two sublattices are equivalent by symmetry. Therefore, we choose to show in the following the results of the sublattices 1 and 3 of the first two cells, i.e. results of the first four layers.

We show in figure 3 the magnetizations and the susceptibilities of sublattices 1 and 3 of the first two cells, in the case where $J_s = -1$.

It is interesting to note that the surface layer has the largest magnetization, followed by that of the second layer, while the third and fourth layers have smaller magnetizations. This is not the case for non-frustrated films, where the surface magnetization is always smaller than the interior ones because of the effects of low-lying energy surface-localized magnon modes [24, 25]. One explanation can be advanced: due to the lack of neighbors, surface spins suffer fluctuations due to the frustration less than the interior spins, so they maintain their ordering up to a higher temperature. Let us decrease the J_s strength. The surface spins then have smaller local field, so thermal fluctuations will reduce their ordering to a lower temperature. Figures 4 and 5 show respectively the cases where $J_s = -0.8$ and -0.5. Near $J_s = -0.8$ the crossover takes place: the surface magnetization becomes smaller than the interior ones for $J_s > -0.8$. Note that the magnetizations of second, third and fourth layers undergo a discontinuity at the transition temperature for $J_s = -0.8$ and -0.5. This suggests that the phase transitions for interior layers are of first order as has been found for a bulk FCC antiferromagnet [15]. This should be checked in the future.

For weak $|J_s|$, there is only one transition for all layers. An example is shown in figure 6 for $J_s = -0.1$. Note that the first-order character disappears as there is no discontinuity of layer magnetizations at the transition temperature.

In the region $-0.5 < J_s < -0.45$, there is an interesting reentrant phenomenon. To facilitate the description of this phenomenon, we show the phase diagram in the space (J_s, T_c) in

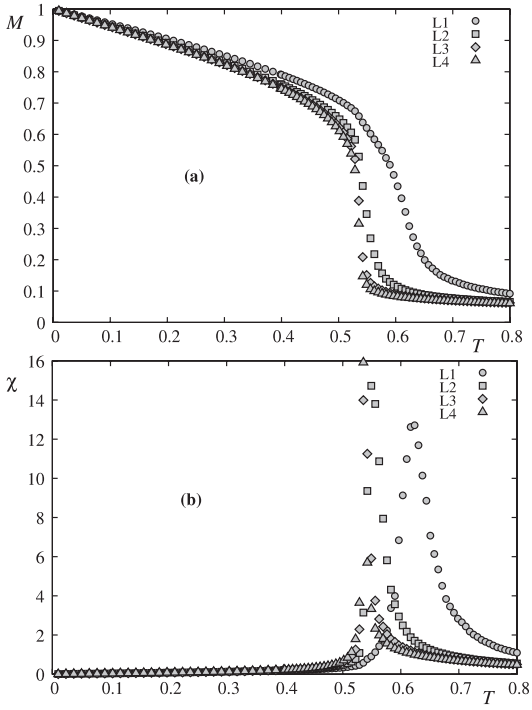

Figure 3. Magnetizations and susceptibilities of sublattices 1 and 3 of the first two cells versus temperature for $J_s = -1.0$ with $L = 24$ and $D = 0.1$. L_j denotes the sublattice magnetization of layer j.

figure 7. In the region $-0.5 < J_s < -0.45$, the GS is of type II, as seen above. According to the phase diagram, we see that, when the temperature increases from zero, the system goes through the phase of type II, and undergoes a transition to enter the phase of type I before making a second transition to the paramagnetic phase at high temperature. This kind of behavior is termed as a reentrant phenomenon, which has been found by exact solutions in a number of very frustrated systems [26, 27]. For a complete review on these exactly solved systems, the reader is referred to the chapter by Diep and Giacomini [28] in [1]. We note here that the reentrance is often found near the frontier where two phases coexist in the GS [1]. This is the case at $J_s = J_s^c = -0.5$.

The discontinued vertical line at $J_s = -0.5$ is a first-order line separating phases I and II. The coexistence of these two phases which do not have the same symmetry explains the first-order character of this line. To show it explicitly, we have calculated at $T = 0.15$ the magnetization M and the staggered magnetization M_{st} of the first layer with varying J_s across -0.5. From the GS configurations shown in figure 2, M should be zero in phase I and finite in phase II, and vice versa for M_{st}. This is observed at $T = 0.15$, as shown in figure 8. The large discontinuity of M and M_{st} at $J_s = -0.5$ shows a very strong first-order character across the vertical line in figure 7.

Let us discuss the finite-size effects in the transitions observed in figures 3 to 6. This is an important question, because it is known that some apparent transitions are artefacts of small system sizes. We have checked with $L = 36$. The results do not change. Of course, we may think that these sizes are still small to change the shape of the phase diagram, especially near $J_s = -0.5$ where finite-size effects may be strong because of the frontier between the two

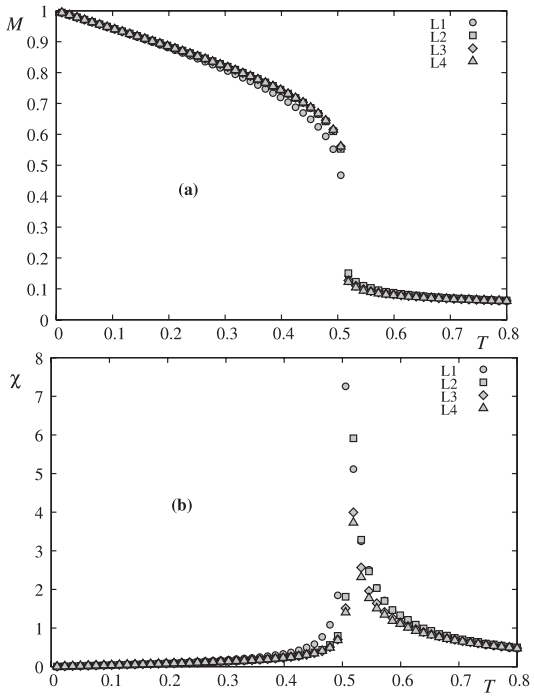

Figure 4. Magnetizations and susceptibilities of sublattices 1 and 3 of the first two cells versus temperature for $J_s = -0.8$ with $L = 24$ and $D = 0.1$. L_j denotes the sublattice magnetization of layer j.

phases. But the results from the Green's function method, which are for infinite L, show, as will be seen later, a similar shape near $J_s = -0.5$. So we believe that the results in figure 7 are correct for infinite size.

To confirm further the observed transitions, we have made a study of finite-size effects on the layer susceptibilities at some chosen values of J_s by using the accurate MC multihistogram technique [29–31].

At this point, let us recall that bulk Ising frustrated systems, unlike unfrustrated counterparts, have different transition natures: the antiferromagnetic FCC and HCP Ising lattices have a strong first-order transition [17–19], while the stacked antiferromagnetic triangular lattice has a controversial nature (see references in [34]). The model studied here is the frustrated FCC film in which surface effects can modify the strong first-order transition observed in its bulk counterpart.

Our results show that transitions at $J_s = -1$ and -0.1 are real second-order transitions obeying some scaling law. Figure 9 shows the size effects on the maximum of the susceptibilities of the first and second layers for $J_s = -0.1$, while figure 10 shows that of the third and fourth layers. As is seen, the maximum of the susceptibilities $\chi^{\max}$ increases with increasing L.

Using the scaling law $\chi^{\max} \propto L^{\gamma/\nu}$, we plot $\ln \chi^{\max}$ versus $\ln L$ in figure 11. The ratio of the critical exponents γ/ν is obtained by the slope of the straight line connecting the data points of each layer.

Within errors the third and fourth layers have the same value of γ/ν, which is neither that of the 2D nor the 3D Ising universality class, 1.75 and 2, respectively. The same occurs

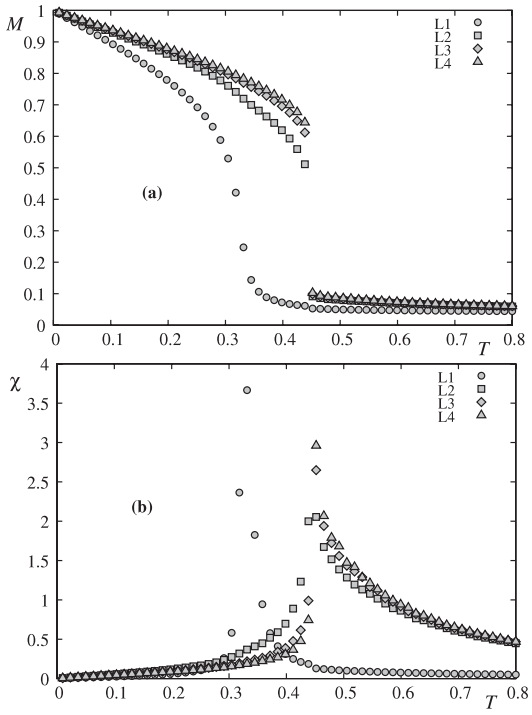

Figure 5. Magnetizations and susceptibilities of the first two cells versus temperature for $J_s = -0.5$ with $L = 24$ and $D = 0.1$. L_j denotes the sublattice magnetization of layer j. The susceptibility of sublattice 1 of the first cell is divided by a factor 5 for presentation convenience.

for the values of the first and second layers. The exponent ν can be obtained as follows. We calculate as a function of T the magnetization derivative with respect to $\beta = (k_B T)^{-1}$: $V_1 = \langle(\ln M)'\rangle = eft\langle E\rangle - \langle ME\rangle / \langle M\rangle$, where E is the system energy and M the sublattice order parameter. We identify the maximum of V_1 for each size L. From the finite-size scaling we know that $V_1^{\max}$ is proportional to $L^{1/\nu}$ [31]. We plot in figure 12 $\ln V_1^{\max}$ as a function of $\ln L$ for $J_s = -0.1$. The slope of each line gives $1/\nu$. For the case $J_s = -0.1$, we obtain $\nu = 0.822 \pm 0.020, 0.795 \pm 0.020, 0.790 \pm 0.020, 0.782 \pm 0.020$ for the first, second, third and fourth layers. These values are far from the 2D value ($\nu = 1$). We deduce $\gamma = 1.510 \pm 0.010, 1.442 \pm 0.015, 1.412 \pm 0.025, 1.395 \pm 0.025$. The values of ν and γ are decreased when one goes from the surface to the interior of the film.

We show in figures 13 and 14 the maximum of sublattice magnetizations and their derivatives for the first two layers in the case of $J_s = -1$. We find $\nu_1 = 0.794 \pm 0.022$, $\nu_2 = 0.834 \pm 0.027$, $\gamma_1 = 1.524 \pm 0.040$, and $\gamma_2 = 1.509 \pm 0.022$.

Let us discuss the values of the critical exponents obtained above. These values do not correspond either to 2D or 3D Ising models ($\gamma_{2D} = 1.75$, $\nu_{2D} = 1$, $\gamma_{3D} = 1.241$, $\nu_{3D} = 0.63$). There are multiple reasons for those deviations. Apart from numerical precision and the modest sizes we used, there may be deep physical origins.

A first question which naturally arises is the effect of the frustration. The 3D version of this model, as said above, has a first-order transition, with a very strong character for the Ising case [17–19] and a somewhat less strong one for the continuous spin models [15]. It has been shown that, at finite temperature, the phenomenon called 'order by disorder' occurs, leading to a reduction of degeneracy: only collinear configurations survive by an entropy effect [15, 32, 33].

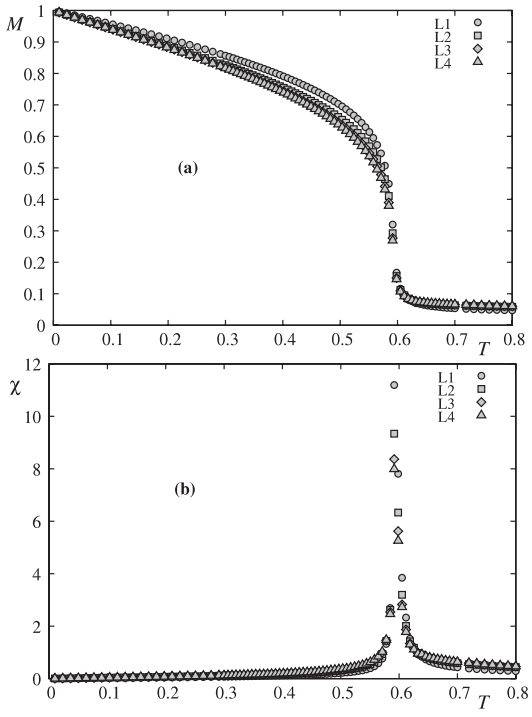

Figure 6. Magnetization and susceptibility of the first two cells versus temperature for $J_s = -0.1$ with $L = 24$ and $D = 0.1$. L_j denotes the sublattice magnetization of layer j.

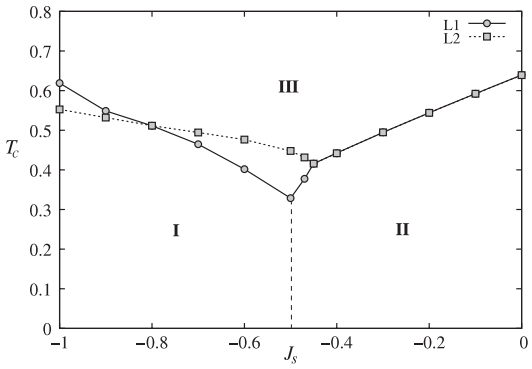

Figure 7. Critical temperature versus J_s with $L = 24$ and $D = 0.1$. L_j denotes data points for the maximum of the sublattice magnetization of layer j. I and II denote ordering of type I and II defined in figure 2. III is a paramagnetic phase. The discontinued vertical line is a first-order line. Errors are smaller than symbol sizes. See text for comments.

The infinite degeneracy is reduced to 6, i.e. the number of ways to put two AF spin pairs on a tetrahedron. The model is equivalent to a 6-state Potts model. The first-order transition observed in the 3D case is in agreement with the Potts criterion according to which the transition in q-state Potts model is of first-order in three dimensions for $q \geqslant 3$.

In the case of a film with finite thickness studied here, it appears that the first-order character is lost.

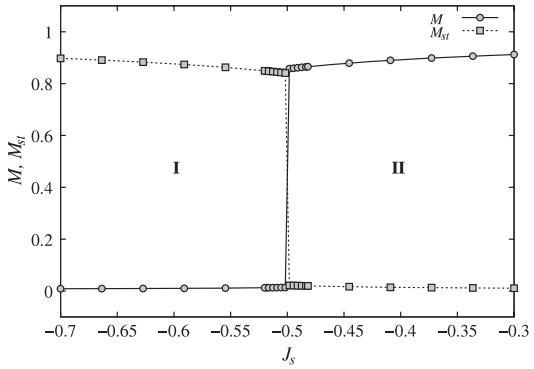

Figure 8. The magnetization M and the staggered magnetization $M_{\rm st}$ of the first layer versus $J_{\rm s}$ are shown, at $T = 0.15$, with $L = 24$ and $D = 0.1$. I and II denote ordering of type I and II, defined in figure 2. III is a paramagnetic phase. See text for comments.

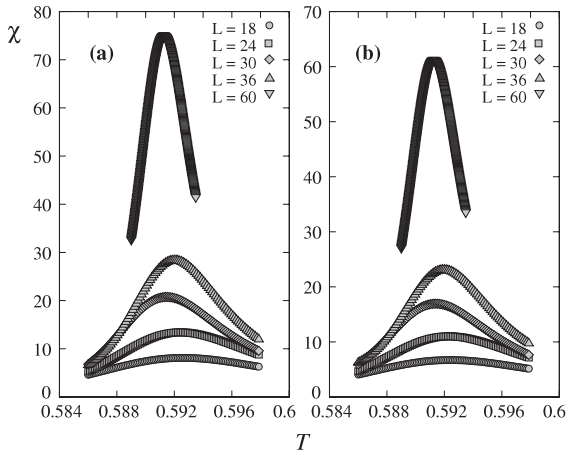

Figure 9. Susceptibilities of layer 1 (left) and 2 (right) are shown for various sizes L as a function of temperature for $J_{\rm s} = -0.1$ and $D = 0.1$.

A first possible cause is from the degeneracy. According to the results shown in the previous section, the GS degeneracy is 2 or 4, depending on $J_{\rm s}$. If we compare to the Potts criterion according to which the transition is of first order in two dimensions only when $q > 4$, then the transition in thin films should be of second order. That is indeed what we observed.

Another possible cause for the second-order transition observed here is from the role of the correlation in the film. For second-order transitions, some arguments, such as those from renormalization group theory, say that the correlation length in the direction perpendicular to the film is finite; hence it is irrelevant to the criticality: the film should have 2D character. If a transition is of first order in three dimensions, i.e. the correlation length is finite at the transition temperature, then in thin films the thickness effect may be important: if the thickness is larger than the correlation length at the transition, than the first-order transition should remain. On the other hand, if the thickness is smaller than that correlation length, the spins then feel an 'infinite' correlation length across the film thickness. As a consequence, two pictures can be thought of: (i) the whole system may be correlated and the first-order character is to become a second-order one, and (ii) the correlation length is longer but still finite; the transition remains of first order.

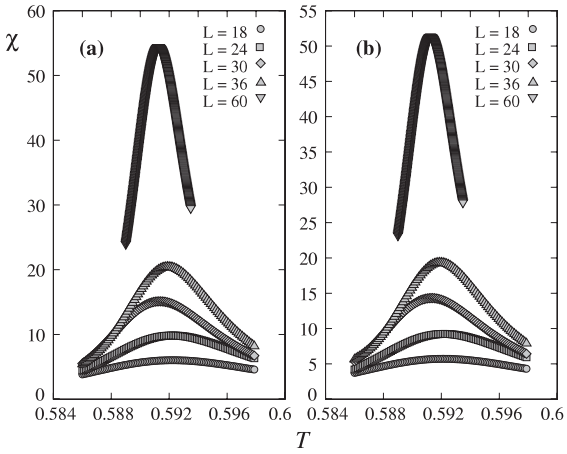

Figure 10. Susceptibilities of layer 3 (left) and 4 (right) are shown for various sizes L as a function of temperature for $J_s = -0.1$ and $D = 0.1$.

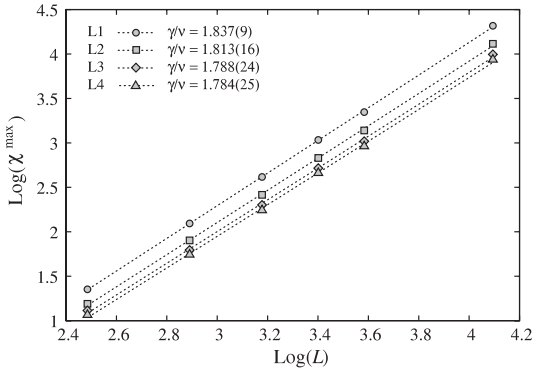

Figure 11. Maximum sublattice susceptibility $\chi^{\max}$ versus L in ln–ln scale, for $J_s = -0.1$ and $D = 0.1$. L_j denotes the sublattice magnetization of layer j. The slopes of these lines give the ratios of exponents γ/ν.

At this point, we would like to emphasize that, in the case of simple surface conditions, i.e. no significant deviation of the surface parameters with respect to those of the bulk, the bulk behavior is observed when the thickness becomes larger than a few dozen atomic layers [24, 25]: surface effects are insignificant on some thermodynamic properties such as the value of the critical temperature, the mean value of magnetization at a given T, etc. It should however be stressed that the criticality is very different. It depends on the correlation length compared to the thickness: for example, we have obtained in the case of simple cubic films with Ising model critical exponents identical to those of the 2D Ising universality class up to thickness of nine layers [35]. Due to the small thickness used here, we think that the 2D character should be assumed.

Now for the anisotropy; remember that in the case studied here, we do not deal with the discrete Ising model but rather an Ising-like Heisenberg model. The deviation from the 2D values may then result in part from a complex coupling between the Ising-like symmetry and the continuous nature of the classical Heisenberg spins. This deviation may be important if the anisotropy constant D is small, as in the case studied here. From the renormalization group

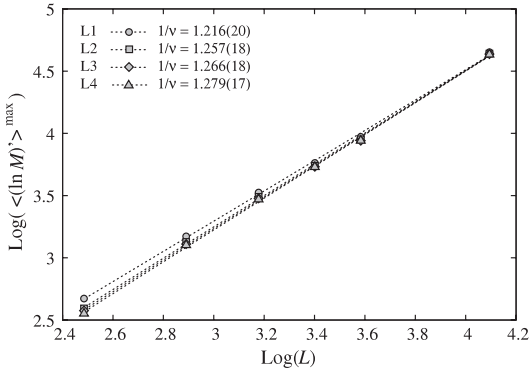

Figure 12. The maximum value of $\langle(\ln M)'\rangle = \langle E\rangle - \langle ME\rangle / \langle M\rangle$ versus L in ln–ln scale for $J_s = -0.1$, where M is the sublattice order parameter. The slope of each line gives $1/\nu$. L_j denotes the sublattice magnetization of layer j.

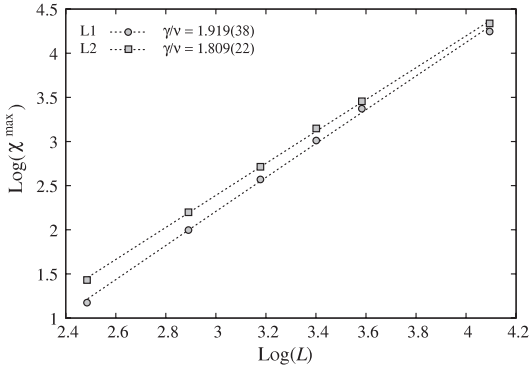

Figure 13. Maximum sublattice susceptibility $\chi^{\max}$ versus L in ln – ln scale, for $J_s = -1$ and $D = 0.1$. L_j denotes the sublattice magnetization of layer j. The slopes of these lines give the ratios of exponents γ/ν.

calculations, since anisotropy is a relevant parameter, one expects that any finite anisotropy will lead to Ising-like critical behavior, but with corrections due to the continuous nature of Heisenberg spins before one enters the linear regime around the Ising fixed point.

To conclude this section, we believe, from the physical arguments given above, that the critical exponents obtained above which do not belong to any known universality class may result from different physical mechanisms. This is a subject of future investigations.

4. Green's function method

We can rewrite the full Hamiltonian (1) in the local framework as

$$\mathcal{H} = -\sum_{\langle i,j\rangle} J_{i,j}\left\{\tfrac{1}{4}(\cos\theta_{ij}-1)(S_i^+S_j^+ + S_i^-S_j^-) + \tfrac{1}{4}(\cos\theta_{ij}+1)(S_i^+S_j^- + S_i^-S_j^+)\right.$$
$$\left. + \tfrac{1}{2}\sin\theta_{ij}(S_i^+ + S_i^-)S_j^z - \tfrac{1}{2}\sin\theta_{ij}S_i^z(S_j^+ + S_j^-) + \cos\theta_{ij}S_i^zS_j^z\right\} - \sum_{\langle i\rangle} I_i(S_i^z)^2, \tag{8}$$

where $\cos(\theta_{ij})$ is the angle between two NN spins.

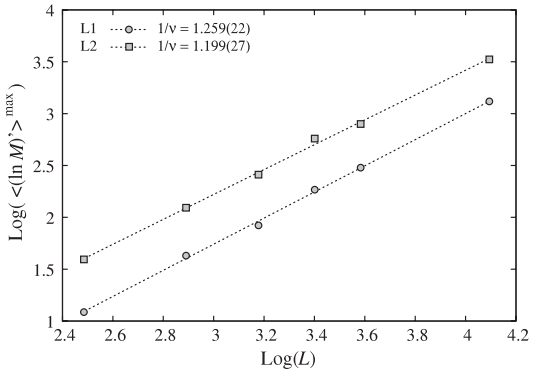

Figure 14. The maximum value of $\langle(\ln M)'\rangle = \langle E\rangle - \langle ME\rangle/\langle M\rangle$ versus L in ln–ln scale for $J_s = -1$, where M is the sublattice order parameter. The slope of each line gives $1/\nu$. $L_k S_j$ denotes one sublattice magnetization of layer j.

To study the properties of quantum spins over a large region of temperatures, there are only a few methods which give relatively correct results. Among them, the GF method is known to recover the exact results at very low T obtained from the spin–wave theory. In addition, it is better than the spin–wave theory at higher temperatures, and can be used up to the transition temperature with of course less precision on the nature of the phase transition. It should be emphasized that the GF method is much better than other methods such as mean-field theories in estimating the value of the critical temperature. We choose this method here to study quantum effects at low T and to obtain the phase diagram at high T.

The GF method can be used for non-collinear spin configurations [36]. In the case studied here, one has a collinear configuration because of the Ising-like anisotropy. In this case, we define two double-time GFs by [37]

$$G_{ij}(t,t') = \langle\langle S_i^+(t);\, S_j^-(t')\rangle\rangle, \tag{9}$$

$$F_{ij}(t,t') = \langle\langle S_i^-(t);\, S_j^+(t')\rangle\rangle. \tag{10}$$

The equations of motion for $G_{ij}(t,t')$ and $F_{ij}(t,t')$ are written by

$$i\frac{\mathrm{d}}{\mathrm{d}t}G_{i,j}(t,t') = \langle[S_i^+(t),\, S_j^-(t')]\rangle\delta(t-t') - \langle\langle[\mathcal{H},\, S_i^+(t)];\, S_j^-(t')\rangle\rangle, \tag{11}$$

$$i\frac{\mathrm{d}}{\mathrm{d}t}F_{i,j}(t,t') = \langle[S_i^-(t),\, S_j^-(t')]\rangle\delta(t-t') - \langle\langle[\mathcal{H},\, S_i^-(t)];\, S_j^-(t')\rangle\rangle. \tag{12}$$

We shall neglect higher-order correlations by using the Tyablikov decoupling scheme [38], which is known to be valid for exchange terms [39]. Then, we introduce the following Fourier transforms:

$$G_{i,j}(t,t') = \frac{1}{\Delta}\int\int \mathrm{d}\mathbf{k}_{xy}\frac{1}{2\pi}\int_{-\infty}^{+\infty}\mathrm{d}\omega\,\mathrm{e}^{-\mathrm{i}\omega(t-t')}.\quad g_{n,n'}\left(\omega,\mathbf{k}_{xy}\right)\mathrm{e}^{\mathrm{i}\mathbf{k}_{xy}\cdot(\mathbf{R}_i-\mathbf{R}_j)}, \tag{13}$$

$$F_{i,j}(t,t') = \frac{1}{\Delta}\int\int \mathrm{d}\mathbf{k}_{xy}\frac{1}{2\pi}\int_{-\infty}^{+\infty}\mathrm{d}\omega\,\mathrm{e}^{-\mathrm{i}\omega(t-t')}.\quad f_{n,n'}\left(\omega,\mathbf{k}_{xy}\right)\mathrm{e}^{\mathrm{i}\mathbf{k}_{xy}\cdot(\mathbf{R}_i-\mathbf{R}_j)}, \tag{14}$$

where ω is the spin–wave frequency, $\mathbf{k}_{xy}$ denotes the wavevector parallel to xy planes, $\mathbf{R}_i$ is the position of the spin at the site i, and n and n' are respectively the indices of the layers to which the sites i and j belong. The integral over $\mathbf{k}_{xy}$ is performed in the first Brillouin zone whose surface is Δ in the xy reciprocal plane.

The Fourier transforms of the retarded GF satisfy a set of equations rewritten under the following matrix form:

$$\mathbf{M}(\omega)\mathbf{g} = \mathbf{u}, \tag{15}$$

where $\mathbf{M}(\omega)$ is a square matrix $(2N_z \times 2N_z)$, and $\mathbf{g}$ and $\mathbf{u}$ are column matrices which are defined as follows:

$$\mathbf{g} = \begin{pmatrix} g_{1,n'} \\ f_{1,n'} \\ \vdots \\ g_{N_z,n'} \\ f_{N_z,n'} \end{pmatrix}, \qquad \mathbf{u} = \begin{pmatrix} 2\langle S_1^z \rangle \delta_{1,n'} \\ 0 \\ \vdots \\ 2\langle S_{N_z}^z \rangle \delta_{N_z,n'} \\ 0 \end{pmatrix}, \tag{16}$$

and

$$\mathbf{M}(\omega) = \begin{pmatrix} A_1^+ & B_1 & D_1^+ & D_1^- & \cdots \\ -B_1 & A_1^- & -D_1^- & -D_1^+ & \vdots \\ \vdots & \cdots & \cdots & \cdots & \vdots \\ \vdots & C_{N_z}^+ & C_{N_z}^- & A_{N_z}^+ & B_{N_z} \\ \cdots & -C_{N_z}^- & -C_{N_z}^+ & -B_{N_z} & A_{N_z}^- \end{pmatrix}, \tag{17}$$

where

$$\begin{aligned} A_n^{\pm} = \omega \pm \big[& \tfrac{1}{2} J_n \langle S_n^z \rangle (Z\gamma)(\cos\theta_n + 1) - J_n \langle S_n^z \rangle Z \cos\theta_n \\ & - 2I_n \langle S_n^z \rangle - 2J_{n,n+1} \langle S_{n+1}^z \rangle \cos\theta_{n,n+1}^{(a)} - 2J_{n,n+1} \langle S_{n+1}^z \rangle \cos\theta_{n,n+1}^{(b)} \\ & - 2J_{n,n-1} \langle S_{n-1}^z \rangle \cos\theta_{n,n-1}^{(a)} - 2J_{n,n-1} \langle S_{n-1}^z \rangle \cos\theta_{n,n-1}^{(b)} \big], \end{aligned} \tag{18}$$

$$B_n = \tfrac{1}{2} J_n \langle S_n^z \rangle (Z\gamma)(\cos\theta_n - 1), \tag{19}$$

$$C_n^{\pm} = J_{n,n-1} \langle S_n^z \rangle \left(\cos\theta_{n,n-1}^{(a)} \pm 1 \right) + J_{n,n-1} \langle S_n^z \rangle \left(\cos\theta_{n,n-1}^{(b)} \pm 1 \right), \tag{20}$$

$$D_n^{\pm} = J_{n,n+1} \langle S_n^z \rangle \left(\cos\theta_{n,n+1}^{(a)} \pm 1 \right) + J_{n,n+1} \langle S_n^z \rangle \left(\cos\theta_{n,n+1}^{(b)} \pm 1 \right), \tag{21}$$

in which, $Z = 4$ is the number of in-plane NNs, $\theta_{n,n\pm1}^{(a)}$ the angle between two NN spins of sublattice 1 and 3 belonging to the layers n and $n \pm 1$ (see figure 2), $\theta_{n,n\pm1}^{(b)}$ the angle between two NN spins of sublattice 1 and 4, θ_n the angle between two in-plane NN spins in the layer n, and

$$\gamma = \frac{1}{Z} \left[4 \cos\left(\frac{k_x a}{2} \right) \cos\left(\frac{k_y a}{2} \right) \right].$$

Here, for compactness, we have used the following notation.

(i) J_n and D_n are the in-plane interactions. In the present model J_n is equal to J_s for the two surface layers and equal to J for the interior layers. All D_n are set to be D.

(ii) $J_{n,n\pm1}$ are the interactions between a spin in the nth layer and its neighbor in the $(n \pm 1)$th layer. Of course, $J_{n,n-1} = 0$ if $n = 1$, $J_{n,n+1} = 0$ if $n = N_z$.

Solving $\det|\mathbf{M}| = 0$, we obtain the spin–wave spectrum ω of the present system. The solution for the GF $g_{n,n}$ is given by

$$g_{n,n} = \frac{|\mathbf{M}|_n}{|\mathbf{M}|}, \tag{22}$$

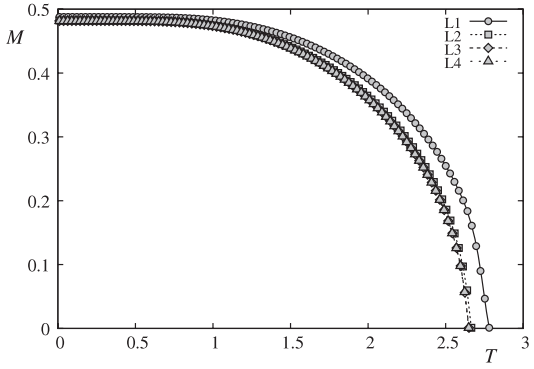

Figure 15. Layer magnetization of the first four layers versus temperature for $J_s = -1.0$ and $D = 4$. L_j denotes the sublattice magnetization of layer j. Note that except for the first layer (upper curve), all other layer magnetizations coincide in this figure scale.

with $|\mathbf{M}|_n$ being the determinant made by replacing the nth column of $|\mathbf{M}|$ by $\mathbf{u}$ in (16). Writing now

$$|\mathbf{M}| = \prod_i \left(\omega - \omega_i\left(\mathbf{k}_{xy}\right)\right), \tag{23}$$

one sees that $\omega_i\left(\mathbf{k}_{xy}\right), i = 1, \ldots, N_z$, are poles of the GF $g_{n,n}$. $\omega_i(\mathbf{k}_{xy})$ can be obtained by solving $|\mathbf{M}| = 0$. In this case, $g_{n,n}$ can be expressed as

$$g_{n,n} = \sum_i \frac{f_n(\omega_i(\mathbf{k}_{xy}))}{(\omega - \omega_i(\mathbf{k}_{xy}))}, \tag{24}$$

where $f_n(\omega_i(\mathbf{k}_{xy}))$ is

$$f_n(\omega_i(\mathbf{k}_{xy})) = \frac{|\mathbf{M}|_n(\omega_i(\mathbf{k}_{xy}))}{\prod_{j\neq i}(\omega_j(\mathbf{k}_{xy}) - \omega_i(\mathbf{k}_{xy}))}. \tag{25}$$

Next, using the spectral theorem which relates the correlation function $\langle S_i^- S_j^+\rangle$ to the GF [40], one has

$$\left\langle S_i^- S_j^+\right\rangle = \lim_{\varepsilon\to 0}\frac{1}{\Delta}\int\int \mathrm{d}\mathbf{k}_{xy}\int_{-\infty}^{+\infty}\frac{i}{2\pi}\big(g_{n,n'}(\omega + \mathrm{i}\varepsilon) - g_{n,n'}(\omega - \mathrm{i}\varepsilon)\big)\cdot\frac{\mathrm{d}\omega}{\mathrm{e}^{\beta\omega}-1}\mathrm{e}^{\mathrm{i}\mathbf{k}_{xy}\cdot(\mathbf{R}_i-\mathbf{R}_j)}, \tag{26}$$

where ϵ is an infinitesimal positive constant and $\beta = 1/k_B T$, k_B being the Boltzmann constant.

Using the GF presented above, we can calculate self-consistently various physical quantities as functions of temperature T. We start the self-consistent calculation from $T = 0$ with a small step for temperature: 5×10^{-3} at low T and 10^{-1} near T_c (in units of J/k_B). The convergence precision has been fixed at the fourth figure of the values obtained for the layer magnetizations. We know from the previous section that the spin configuration is collinear; therefore, in this section, we shall use a large value of Ising anisotropy D in order to get a rapid numerical convergence. For numerical calculation, we will use $D = 4$ and $J = -1$ and a size of 80^2 points in the first Brillouin zone.

Figure 15 shows the sublattice magnetizations of the first four layers. As seen, the first-layer one is larger than the other three just as in the case of the classical spins shown in figure 3. This difference in sublattice magnetization between layers vanishes at $J_s \simeq -0.8$, as seen in

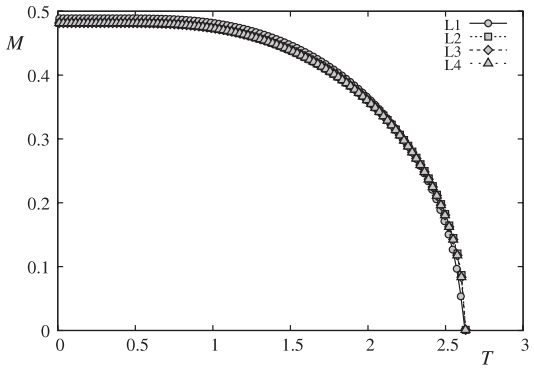

Figure 16. Layer magnetizations of the first four layers versus temperature for $J_s = -0.8$ and $D = 4$. L_j denotes the sublattice magnetization of layer j. Note that except for the first layer at low T (upper curve), all other layer magnetizations coincide in this figure scale.

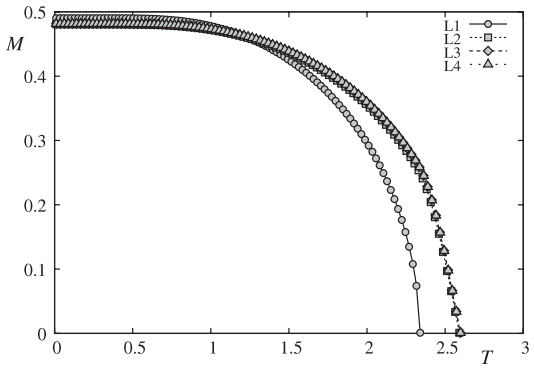

Figure 17. Layer magnetization of the first four layers versus temperature for $J_s = -0.5$ and $D = 4$. L_j denotes the sublattice magnetization of layer j. Note that the first layer makes a crossover: it is higher at low T and smaller at high T than all other layer magnetizations which coincide in this figure scale. See text for comments on the crossover of surface magnetization.

figure 16. Again here, one has a good agreement with the case of classical spins shown in figure 4.

For $J_s > -0.8$, the sublattice magnetization of the first layer is larger at low T and higher at high T, as seen in figure 17 for $J_s = -0.5$. This crossover of sublattice magnetizations comes from the competition between quantum fluctuations and the strength of J_s: when $|J_s|$ is small, the quantum fluctuations of the surface layer are small, yielding a small zero-point spin contraction for surface spins at $T = 0$. So, the surface magnetization is higher than the interior ones. At higher T, however, small $|J_s|$ gives rise to a small local field for surface spins, which in turn yields a smaller surface magnetization at high T. This crossover has been found earlier in antiferromagnetic superlattices and films [41, 42].

For $J_s = -0.1$, there is no longer a crossover at low T, as seen in figure 18. Moreover, there is only a single transition at $T_c \simeq 2.65$ for both surface and interior layers.

We summarize in figure 19 the phase diagram for the quantum spin case obtained with the GF method. The vertical discontinued line indicates the boundary between ordered phases of types I and II. Phase III is paramagnetic. Note the following interesting points:

(i) for $J_s < -0.4$ there is a surface transition distinct from that of interior layers;

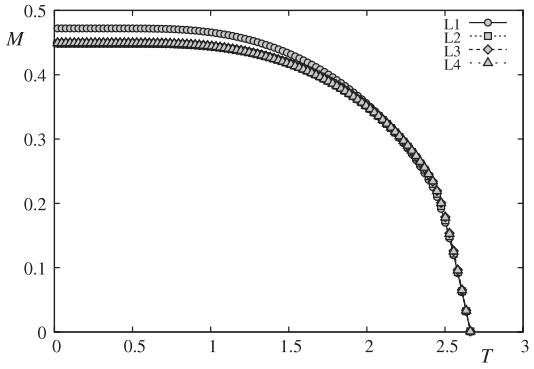

Figure 18. Layer magnetization of the first four layers versus temperature for $J_s = -0.1$ and $D = 4$. L_j denotes the sublattice magnetization of layer j. Only at low T is the surface magnetization distinct (upper curve) from the other ones.

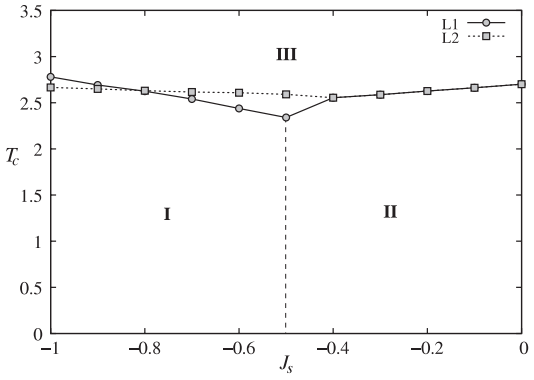

Figure 19. Phase diagram obtained by the Green's function method with $D = 4$. L_j denotes the transition temperature of the sublattice magnetization of layer j. Errors are smaller than the symbol sizes. See text for comments.

(ii) for $J_s < -0.8$, a surface transition occurs at a temperature higher than that of interior layers;

(iii) there is a reentrance between $J_s = -0.4$ and -0.5. This is very similar to the phase diagram of the classical spins obtained by MC simulations shown in figure 7.

5. Concluding remarks

We have studied in this paper the properties of a thin film made from a fully frustrated material, namely an FCC antiferromagnet. We have considered both classical and quantum Heisenberg spin models with an Ising-like single-ion anisotropy. The classical case was treated by Monte Carlo simulation while the quantum case was studied by the Green's function method. Several important results are found in this paper. We found that the presence of a surface reduces the GS degeneracy of the fully frustrated FCC antiferromagnet and there exists a critical value of the in-plane surface interaction $J_s^c = -0.5$ which separates the GS configuration of type I from that of type II. We have studied the phase transition of the system. The surface spin ordering is destroyed in general at a temperature different from that of the interior layers. We

found that in a small region just above J_s^c there is a reentrant phase: with decreasing T the system first changes from the paramagnetic phase to the type II phase, and then enters at a lower temperature into the type I phase. The critical behaviors of surface and interior layers have been shown and discussed.

We hope that these unusual surface properties will help experimentalists to analyze their data obtained for real systems in which frustration plays an important role.

Acknowledgments

VTN thanks the 'Asia Pacific Center for Theoretical Physics' (South Korea) for financial post-doctoral support and hospitality during the period 2006–2007 when part of this work was carried out.

References

[1] See reviews on theories and experiments given in Diep H T (ed) 2005 *Frustrated Spin Systems* (Singapore: World Scientific)
[2] Zangwill A 1988 *Physics at Surfaces* (Cambridge: Cambridge University Press)
[3] Bland J A C and Heinrich B (ed) 1994 *Ultrathin Magnetic Structures* vol I and II (Berlin: Springer)
[4] Binder K 1983 *Phase Transitions and Critical Phenomena* vol 8, ed C Domb and J L Lebowitz (London: Academic)
[5] Diehl H W 1986 *Phase Transitions and Critical Phenomena* vol 10, ed C Domb and J L Lebowitz (London: Academic)
Diehl H W 1997 *Int. J. Mod. Phys.* B **11** 3503
[6] Baibich M N, Broto J M, Fert A, Nguyen Van Dau F, Petroff F, Etienne P, Creuzet G, Friederich A and Chazelas J 1988 *Phys. Rev. Lett.* **61** 2472
[7] Grunberg P, Schreiber R, Pang Y, Brodsky M B and Sowers H 1986 *Phys. Rev. Lett.* **57** 2442
Binash G, Grunberg P, Saurenbach F and Zinn W 1989 *Phys. Rev.* B **39** 4828
[8] Barthélémy A *et al* 2002 *J. Magn. Magn. Mater.* **242–245** 68
[9] See review by Tsymbal E Y and Pettifor D G 2001 *Solid State Physics* vol 56 (San Diego, CA: Academic) pp 113–237
[10] See Ngo V T, Viet Nguyen H, Diep H T and Lien Nguyen V 2004 *Phys. Rev.* B **69** 134429 and references on magnetic multilayers cited therein
[11] See Ngo V T and Diep H T 2007 *Phys. Rev.* B **75** 035412 and references on surface effects cited therein
[12] Kaplan T A and Menyuk N *Phil. Mag.* **87** 3711–85 and references therein
[13] Oguchi T, Nishimori H and Taguchi Y 1985 *J. Phys. Soc. Japan* **54** 4494
[14] Lallemand P, Diep H T, Ghazali A and Toulouse G 1985 *J. Physique Lett.* **46** L1087
[15] Diep H T and Kawamura H 1989 *Phys. Rev.* B **40** 7019
[16] Gvozdikova M V and Zhitomirsky M E 2005 *JETP Lett.* **81** 236
[17] Lebowitz J L and Kalos M H 1980 *Phys. Rev.* B **21** 4027
[18] Polgreen T L 1984 *Phys. Rev.* B **29** 1468
[19] Styer D F 1985 *Phys. Rev.* B **32** 393
[20] Diep H T 1992 *Phys. Rev.* B **45** 2863 and references therein
[21] Mermin N D and Wagner H 1966 *Phys. Rev. Lett.* **17** 1133
[22] Landau D P and Binder K 1990 *Phys. Rev.* B **41** 4786
[23] Binder K, Landau D P and Ferrenberg A M 1995 *Phys. Rev.* E **51** 2823
[24] Diep H T, Levy J C S and Nagai O 1979 *Phys. Status Solidi* b **93** 351
[25] Diep H T 1981 *Phys. Status Solidi* b **103** 809
[26] Diep H T, Debauche M and Giacomini H 1991 *Phys. Rev.* B **43** 8759 (rapid communication)
[27] Debauche M, Diep H T, Giacomini H and Azaria P 1991 *Phys. Rev.* B **44** 2369
[28] Diep H T and Giacomini H Frustration—exactly solved frustrated models in [1] (chapter)
[29] Ferrenberg A M and Swendsen R H 1988 *Phys. Rev. Lett.* **61** 2635
[30] Ferrenberg A M and Swendsen R H 1989 *Phys. Rev. Lett.* **63** 1195
[31] Ferrenberg A M and Landau D P 1991 *Phys. Rev.* B **44** 5081
[32] Villain J, Bideaux R, Carton J P and Conte R 1980 *J. Physique* **41** 1263

[33] Henley C 1987 *J. Appl. Phys.* **61** 3962
Henley C 1989 *Phys. Rev. Lett.* **62** 2056
[34] Plumer M L, Mailhot A, Ducharme R, Caillé A and Diep H T 1993 *Phys. Rev.* B **47** 14312
[35] Tu X T, Ngo V T and Diep H T 2007 unpublished
[36] See for example Quartu R and Diep H T 1997 *Phys. Rev.* B **55** 2975
Santamaria C, Quartu R and Diep H T 1998 *J. Appl. Phys.* **84** 1953
[37] Tahir-Kheli R A and Ter Haar D 1962 *Phys. Rev.* **127** 88
[38] Bogolyubov N N and Tyablikov S V 1959 *Dokl. Akad. Nauk SSSR* **126** 53
Bogolyubov N N and Tyablikov S V 1959 *Sov. Phys.—Dokl.* **4** 604 (Engl. Transl.)
[39] Fröbrich P, Jensen P J and Kuntz P J 2000 *Eur. Phys. J* B **13** 477 and references therein
[40] Zubarev D N 1960 *Usp. Fiz. Nauk* **187** 71
Zubarev D N 1960 *Sov. Phys.—Usp.* **3** 320 (Engl. Transl.)
[41] Diep H T 1989 *Phys. Rev.* B **40** 4818
[42] Diep H T 1991 *Phys. Rev.* B **43** 8509